

SPECTROGRAM ANALYSIS OF CIRCUMFERENTIAL MODES PROPAGATING AROUND THE CIRCULAR CYLINDRICAL SHELL IMMERSSED IN WATER

M. Laaboubi¹, A. Dliou^{1,2}, R. Latif^{1,2}, E. Aassif¹, G. Maze³

¹ LMTI, Laboratoire de Métrologie et Traitement d'Information, Ibn Zohr University, Agadir, Morocco,

² ESSI-ENSA, École Nationale des Sciences Appliquées, Ibn Zohr University, Agadir, Morocco,

³ LOMC, Laboratoire Ondes et Milieux Complexes FRE CNRS 3201, Le Havre University, Le Havre, France.

ABSTRACT

In this study, we show that the characterization of an elastic tube can be made from the cut-off frequencies of the circumferential waves and the wave velocities in the material constituting the tube. The time-frequency spectrogram is applied to an acoustic signal backscattered by an Aluminum tube for identification of circumferential wave. The cut-off frequencies of the each circumferential wave modes such as A_1 , A_2 (Antisymmetric modes) and S_1 (Symmetric mode) are estimated from the spectrogram images, and are compared with those calculated via the normal modes theory. The transverse and the longitudinal velocities of Aluminum material, determined from the spectrogram images, are in good agreement with those given in the scientific literature.

RESUME

Dans ce travail, nous exposons la possibilité de mettre œuvre la caractérisation d'un tube élastique à partir de la fréquence de coupure des ondes circonférentielles et des vitesses des ondes propageant dans le matériau constituant le tube. La représentation temps-fréquence de Spectrogramme est appliquée à un signal acoustique rétrodiffusé par un tube d'Aluminium afin de pouvoir identifier les ondes circonférentielle. La fréquence de coupure de chaque mode d'onde circonférentielle tels que : A_1 , A_2 (modes antisymétriques) et S_1 (mode symétrique) sont estimées à partir des images temps-fréquence de Spectrogramme puis elles sont comparées avec celles calculées par la théorie des modes propres. Les vitesses transversales et longitudinales du matériau en Aluminium, déterminées à partir des images temps-fréquence, sont en bon accord avec celles données dans la littérature scientifique.

1. INTRODUCTION

Previous theoretical and experimental studies on the acoustic scattering field have shown that the acoustic resonances of a simple shape target (plate, cylinder, tube...) depend on its physical and geometrical characteristics. The analysis of the acoustic signals backscattered by a target is done either in the frequency domain using the Fourier transform (backscattered spectrum and/or resonance spectrum) or in the time domain (observation of the form and the periodicity of the echoes) [1-12]. These two one-dimensional representations prove to be insufficient to visualize the frequential components evolution versus the time, to observe the circumferential waves trajectories and obtain directly their cut-off frequencies. Latif et. al. have analyzed the signal by the time-frequency Wigner-Ville representation which takes into consideration both the time t and frequency f of the acoustic signal [13]. This analysis is focused to determine the cut-off frequency of the circumferential anti-symmetric wave A_1 and study the evolution of this frequency as a function of the radius ratio b/a of a tube (b : internal radius and a : external radius).

The present paper is especially concerned with the application of an alternate time-frequency representation called Spectrogram. The new study will extend the work started on an earlier study by the time-frequency Wigner-Ville technique and improve

the limitation of the earlier study of Refeerncfe13. The time-frequency spectrogram representation has been chosen as it will decrease the number of cross-term components, a principal drawback of the time-frequency Wigner-Ville technique [14-22]. The new representation has been used to determine the cut-off frequency of circumferential waves such as A_1 , A_2 (Antisymmetric modes) and S_1 (Symmetric mode) and calculate the transverse and longitudinal velocities of the tube material.

The spectrogram representation allows one to obtain a synthetic circumferential waves dispersion image and determine, directly, physical and geometrical parameters. The spectrogram representation is applied to analyze a theoretical acoustic signal backscattered by an aluminum tube of radius ratio b/a immersed in water. The aim of this study was to test the spectrogram effectiveness and accuracy in determining the circumferential wave cut-off frequencies as well as to compare the transverse and the longitudinal velocities derived from the spectrogram analysis with those derived from the theory. When the wall of the cylindrical shell is thin (radius ratio b/a tends to 1) the circumferential waves are identical to the Lamb waves [23-29]. The cut-off frequencies of these waves are first determined from the spectrogram image and then the velocities of these waves of the tube material are then calculated. These velocities are then compared with those calculated by the normal modes theory [13, 30].

2. THEORETICAL BACKGROUND

2.1 Time-frequency representation of the spectrogram

The Short Time Fourier Transform (STFT) can be interpreted as a Fourier analysis of successive sections of the signal weighted by a temporal window such as Gabor, Hamming, and Blackman. The expression of the STFT is given by [14,15,31,32]:

$$STFT(t, f) = \int_{-\infty}^{+\infty} s(\tau) h_{t,f}^*(\tau) d\tau = \int_{-\infty}^{+\infty} s(\tau) h^*(\tau-t) e^{-2\pi i f \tau} d\tau \quad (1)$$

where, $h_{t,f}^*(\tau)$ is the complex conjugate of the analysis window $h_{t,f}(\tau)$, t the time, f the frequency, τ the integral variable, $s(t)$ the temporal signal. This relation represents the scalar product between the signal $s(t)$ and the function $h_{t,f}(\tau)$. In practice, the Spectrogram (SP) is the squared modulus of the STFT and is given by [14, 15,17,18]:

$$SP(t, f) = |STFT(t, f)|^2 \quad (2)$$

The integral of the $SP(t, f)$ with respect to the frequency yields produces the instantaneous signal power P [15]:

$$P = \int_{-\infty}^{+\infty} SP(t, f) df = |s(t)|^2 \quad (3)$$

The time integral of the $SP(t, f)$ produces the signal power density spectrum D :

$$D = \int_{-\infty}^{+\infty} SP(t, f) dt = |S(f)|^2 \quad (4)$$

where $S(f)$ is the Fourier transform of the signal $s(t)$.

With regard to numerical calculations, one won't be able to reach the true spectrogram distribution. To resolve this problem, numerically, we use the discrete time version of this distribution SP_s . The distribution expression is given by [14,15]:

$$SP_s(n, f) = \left| \sum_{k=-N+1}^{N-1} h^*[k] s[n+k] e^{-2\pi i f k} \right|^2 \quad (5)$$

where n is the sampled time, $2N+1$ is the smooth window length and $k = -N+1, \dots, N-1$.

2.2. Acoustic scattering by an elastic cylinder

The study of the acoustic scattering by targets of simple geometrical shape is the object of many works [1-12]. In this paper we will use a plane harmonic wave incident on an infinite tube of radius ratio, b/a , with an air-filled cavity (Fig. 1). The mathematical approach of impulse response of tube is based on the

Rayleigh series formations that consist in the decomposition of the backscattered pressure field into infinite sum of modal components [8], depending on both the mechanical properties and the geometry of the target.

The general geometry for the backscattering of a plane wave by a tube is illustrated in Figure 1.

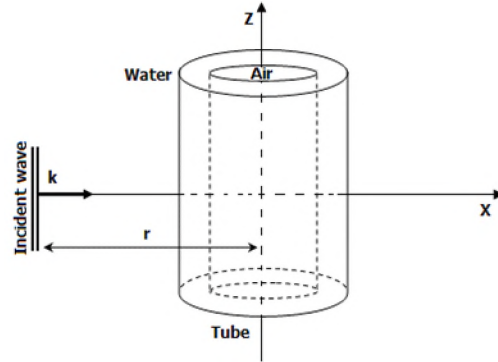


Figure 1. Problem Geometry.

The mechanisms of the echo formation of the circumferential waves and the Scholte wave are shown in Figure 2 [33,34]. Scholte waves are acoustic waves propagating at a fluid/solid interface. They are localized in the neighborhood of the phase boundary in the sense that they decay exponentially in both directions along the normal to the interface [35].

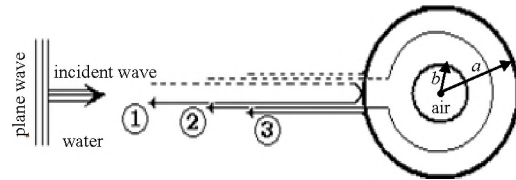


Figure 2. Mechanisms of the echo formation
(1- specular reflection, 2- circumferential waves and 3- Scholte wave)

The different echoes, of the circumferential waves and the Scholte wave presented in the Figure 2, constitute the backscattering complex pressure. This complex pressure in far field of the cylindrical shell immersed in water (Fig. 1) is given by the expression [1,4]:

$$P_{scat}(\omega) = P_0 \sum_{n=0}^{\infty} \frac{D_n^{[1]}(\omega)}{D_n(\omega)} H_n^{(1)}(kr) \quad (6)$$

where ω is angular frequency, $k = \omega/c$ is the wave number with respect to wave velocity in the external fluid and c is the sound velocity in water. P_0 is the plane incident wave amplitude and r is the receiver position. $D_n(\omega)$ and $D_n^{[1]}(\omega)$ are determinants computed from the boundary conditions of the problem (continuity of radial stress and

displacements of both interfaces). $H_n^1(kr)$ is the Hankel function of the first kind.

With the mechanism above (Fig. 2), we store the backscattering complex pressure P_{scat} , as illustrated in Figure 4.

2.3 Lamb wave dispersion

In this work, we have used a thin tube with radius ratio $b/a=0.95$ close to 1. From the similarities between the plates and the thin tubes with the same thickness we have used the dispersion curves relationships of the lamb wave propagating in the plate [13,30,36]. Figure 3 presents the dispersion curves of symmetric and antisymmetric Lamb waves in an aluminum plate.

The phase velocity is calculated from the resonance frequencies that correspond to Lamb waves propagating in the plate. Thus from each resonance frequency, an integer number of wavelengths fits the thickness of the plate, and the following relation holds [35]:

$$C_{ph}(f) = \frac{2\pi fe}{n} \quad (7)$$

where n is the Lamb wave mode.

The function of the dimensionless frequency ka is defined by the expression below [2,9]:

$$ka = \frac{2\pi fa}{c} \quad (8)$$

For a thin tube wall, it can be shown that the plate Lamb wave and the tube circumferential wave are similar at very low frequencies [37]. The reduced frequency $fe/2$ (where $(fe/2)$ is the frequency-thickness product for a plate in MHz, e is the plate thickness in mm ($e=a-b$)) used to calculate these curves are related to the dimensionless frequency used in the case of cylindrical shell with the relation [13,30]:

$$ka = \frac{4\pi}{c(1-\frac{b}{a})} f \frac{e}{2} \quad (9)$$

Due to the similarity between the circumferential waves and Lamb waves, it is possible to use the classical relations on the Lamb waves. These relations allow us to determine the value of the cut-off frequency of the circumferential wave in the case of a tube [37-39]. In the case of a thin plate, the cut-off frequencies of the symmetric and anti-symmetric Lamb waves are provided, respectively using the dispersion curve of Lamb wave on a plate [13,20-22]:

$$fe = \begin{cases} m_s c_T \\ (m_s + \frac{1}{2}) c_L \end{cases} \quad (10)$$

$$fe = \begin{cases} m_a c_L \\ (m_a + \frac{1}{2}) c_T \end{cases} \quad (11)$$

where c_T and c_L are transverse and longitudinal velocities of the material constituting the tube. m_s and m_a are the integer numbers indicating symmetric and anti-symmetric modes of plate vibrations respectively. From equations (9), (10) and (11) we determine the relation between the cut-off frequencies (ka) and the transverse velocity c_T and the longitudinal velocity c_L .

$$ka = \frac{2\pi}{c(1-\frac{b}{a})} \begin{cases} m_s c_T \\ (m_s + \frac{1}{2}) c_L \end{cases} \quad (12)$$

$$ka = \frac{2\pi}{c(1-\frac{b}{a})} \begin{cases} m_a c_L \\ (m_a + \frac{1}{2}) c_T \end{cases} \quad (13)$$

The cut-off frequency of the A1, S2, S1 and A2 Lamb waves are calculated with the relation (10) and (11) determined from Figure 3 (the cut-off frequency of each Lamb wave is indicated by a vertical arrow). Table 1 gives these cutoff frequencies and their relations with the cutoff frequencies observed in the case of cylindrical shells, calculated with the relation (9).

3. Method

3.1 The backscattering spectrum

Figure 4 illustrates the theoretical backscattering spectrum of an air-filled aluminum tube immersed in water, which is obtained theoretically by the expression (6).

3.2 The synthetic time-domain signal and the resonance spectrum

The backscattering spectrum in Figure 4 shows that it is broad-band in nature but with abrupt shape transitions corresponding to resonances.

The time signal $S(t)$ of a tube is calculated by the inverse Fourier transform of the backscattering spectrum.

$$s(t) = \frac{1}{2\pi} \int_{-\infty}^{+\infty} h(\omega) P_{scat}(\omega) e^{i\omega t} d\omega \quad (8)$$

where $h(\omega)$ is the pass-band of the transducer.

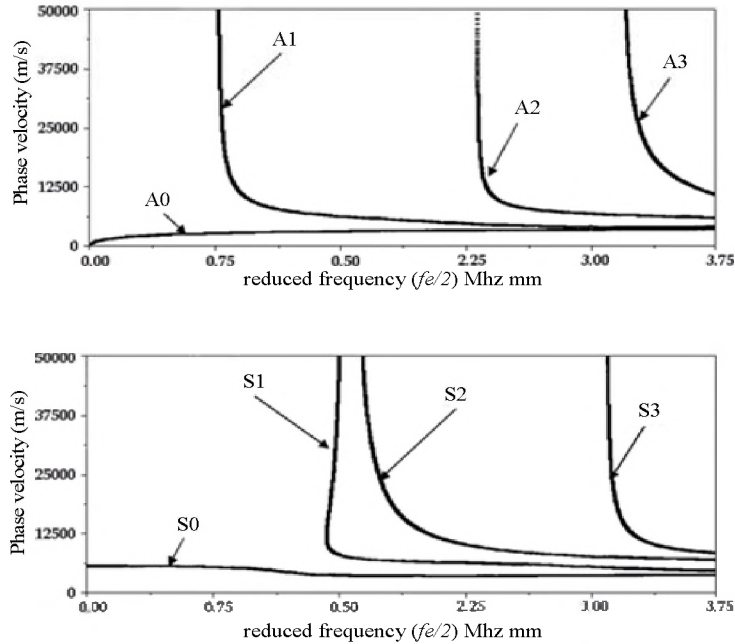


Figure 3. Dispersion curves of symmetric and antisymmetric Lamb waves in an aluminum plate

Table 1. Cutoff frequency of Lamb waves in plate and in cylindrical shells (m_a and m_s are integer numbers)

Lamb wave type	Form vibration modes	$fe/2$ (MHz mm)	ka
A1	$m_a=1$ 	0.775 ± 0.020	132.24 ± 3.41
S1	$m_s=1$ 	1.550 ± 0.020	264.87 ± 3.41
S2	$m_s=2$ 	1.595 ± 0.020	272.56 ± 3.41
A2	$m_a=2$ 	2.325 ± 0.020	397.30 ± 3.41

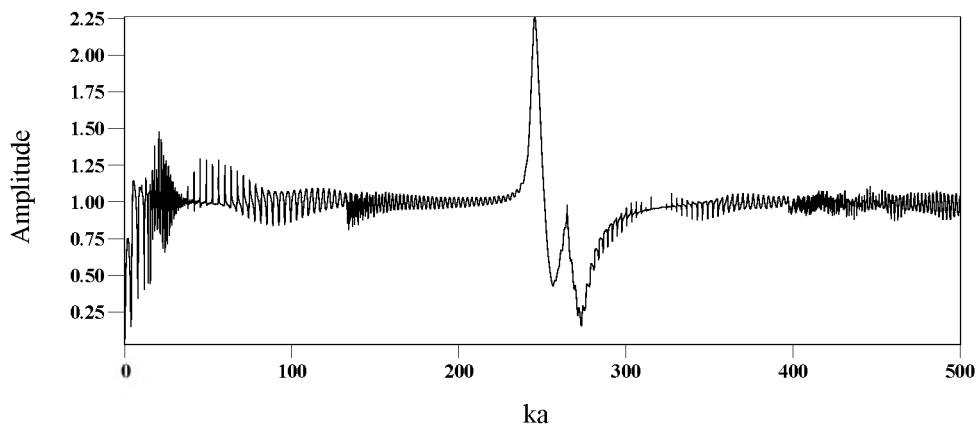


Figure 4. Backscattering spectrum of an air-filled aluminum cylindrical shell immersed in water, $b/a = 0.95$, $a=3\text{cm}$.

The resonance spectrum is obtained as follows: first a theoretical temporal signal is calculated from the backscattered spectrum with an inverse Fourier transform, it corresponds to the time signal observed when the tube is excited with a broadband impulse (Fig. 5a); on this time signal, various echoes related to the circumferential waves are observed, second the specular echo related to the reflection on the tube is deleted with a Personal Computer and replaced by

zeros (Fig. 5b); third a new Fourier transform is applied to the filtered time signal. The resulting resonance spectrum is shown in Figure 6. For each transition in Figure 4, a peak resonance is observed in Figure 6. Resonances which appear on the backscattering resonance spectrum (Fig. 6) are related to the circumferential waves propagating around the tube circumference [40].

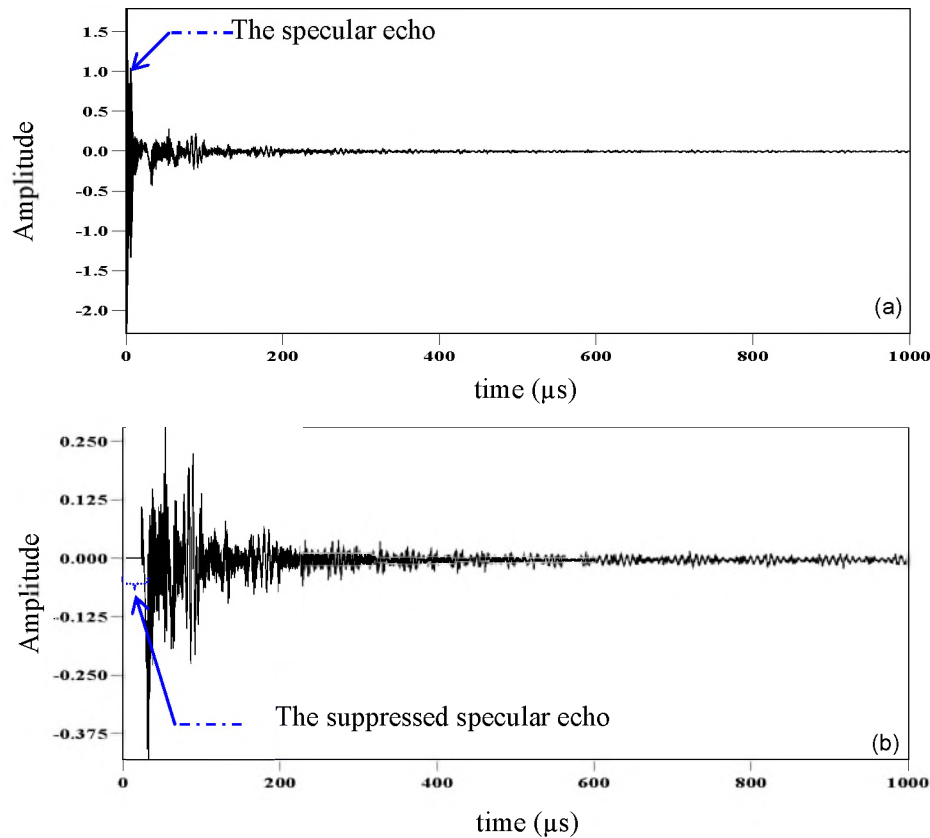


Figure 5. Temporal signal of an aluminum tube $b/a=0.95$, (a) is the global signal and (b) is the signal (a) with deleted specular echo.

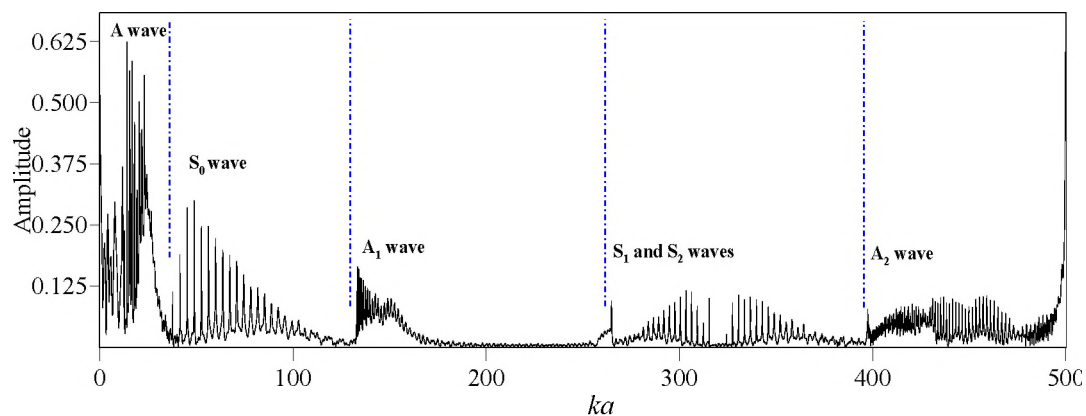


Figure 6. Resonance spectrum of an air-filled aluminum cylindrical shell immersed in water, $b/a = 0.95$, $a=3\text{cm}$.

Different families of resonances are observed from Figure 6, such as,

- A1 wave resonances at frequency, $ka = 132$,
- S1 wave resonances at frequency, $ka = 260$,
- S2 wave resonances at frequency, $ka = 270$,
- A2 wave resonances at frequency, $ka = 397$.

3.3 Spectrogram images

The time-frequency method is a representation that allows a two dimensional characterization of the

signal projection. Thus, one can follow the spectrum content's temporal evolution of the circumferential waves propagating around the tube circumference [4,21,22]. The spectrogram distribution from Eq. 5 is applied to the temporal signal backscattered by an air-filled aluminum tube with $b/a = 0.95$.

Figure 7 shows the time-frequency spectrogram image of the theoretical temporal signal using a Blackman window of 200 points (Fig. 5b). This representation illustrates the synthetic image of the multimode related to the circumferential waves such as S_0 , A_1 , S_1 , S_2 and A_2 which appear in the signal.

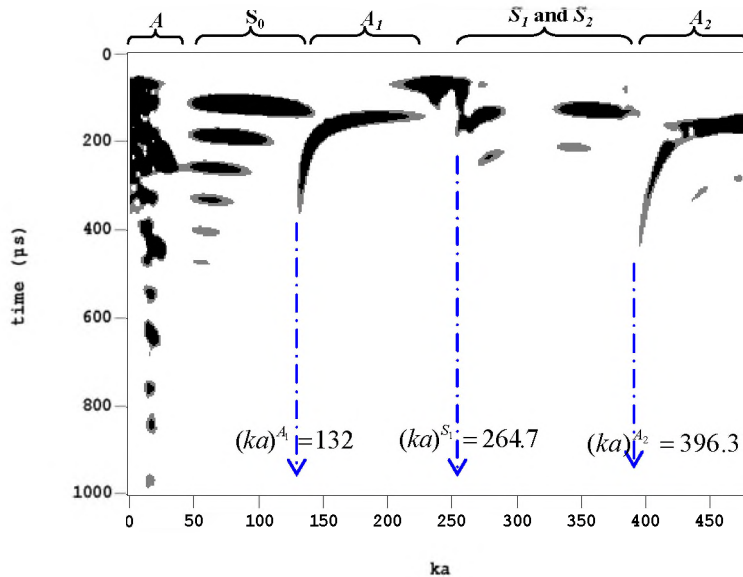


Figure 7. Spectrogram time-frequency image of the theoretical temporal signal (Blackman window of the 200 points).

Applying a digital filter on the spectrum (Figure 6), allow us to extract the spectrum for each circumferential wave mode. The application of the inverse Fourier transform to different spectrums acquired by the digital filtering provides temporal signals corresponding to different mode wave (Figures 8.a, 9.a, 10.a and 11.a). Figures 8, 9, 10 and 11 present the spectrogram synthetic images for the anti-symmetric and symmetric waves S_0 , A_1 , S_1 and A_2 respectively with Blackman window of 200 points.

These figures present also the original temporal signals (figures 8a, 9a, 10a and 11a), from which the Spectrogram images were obtained (figures 8b, 9b, 10b and 11b), and the resonance spectrums correspondents (figures 8c, 9c, 10c and 11c).

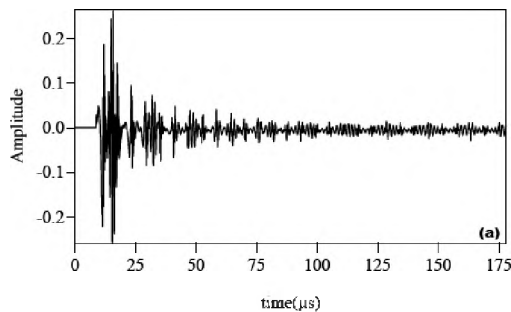


Figure 8 (a) Time Signal of Scholte A and the symmetric S_0 waves

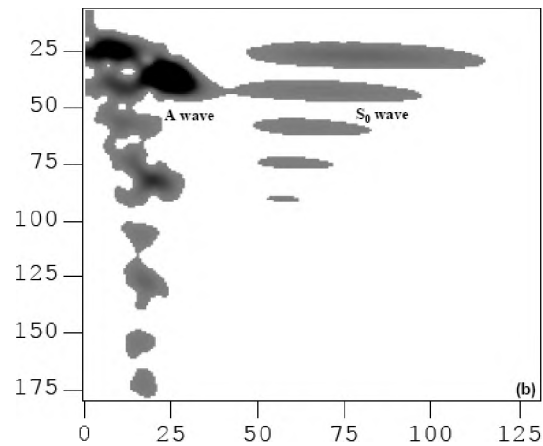


Figure 8 (b) Spectrometric Image of Scholte A and the symmetric S_0 waves

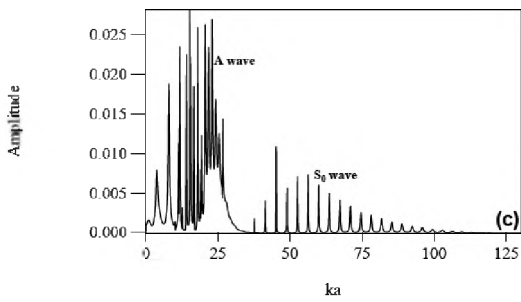


Figure 8 (c) Resulting Resonance Spectra of Scholte A and the symmetric S_0 waves

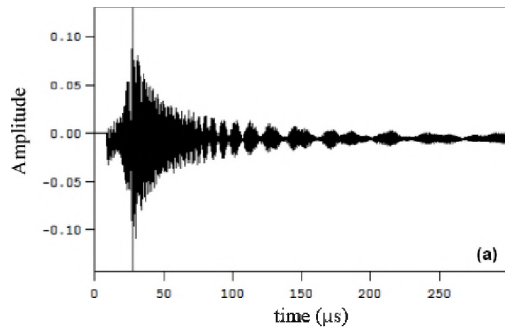


Figure 9 (a) Time Signal of the antisymmetric A_1 wave

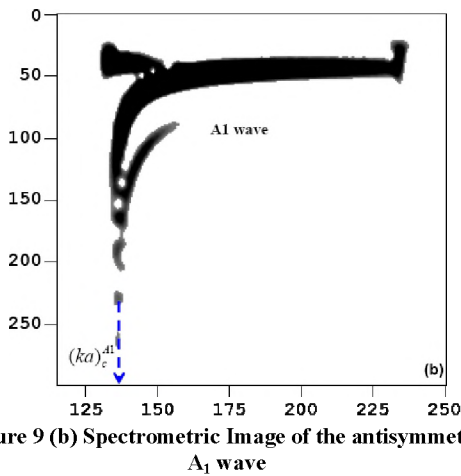


Figure 9 (b) Spectrometric Image of the antisymmetric A_1 wave

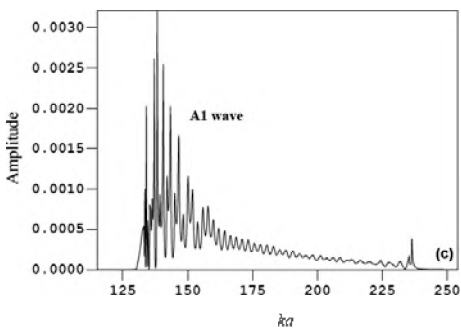


Figure 9 (c) Resulting Resonance Spectra of the antisymmetric A_1 wave

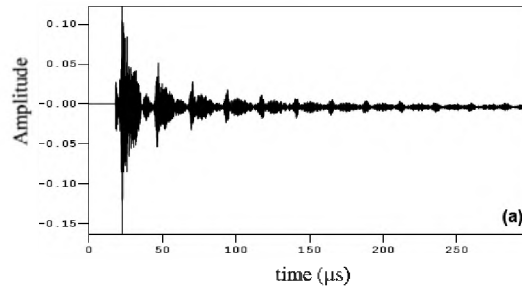


Figure 10 (a) Time Signal of the symmetric S_1 wave

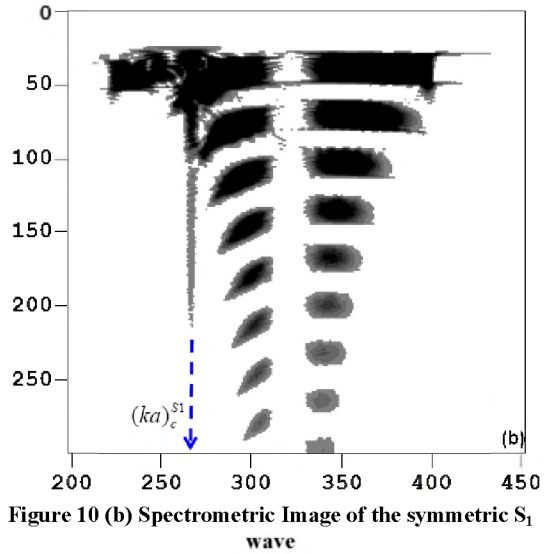


Figure 10 (b) Spectrometric Image of the symmetric S_1 wave

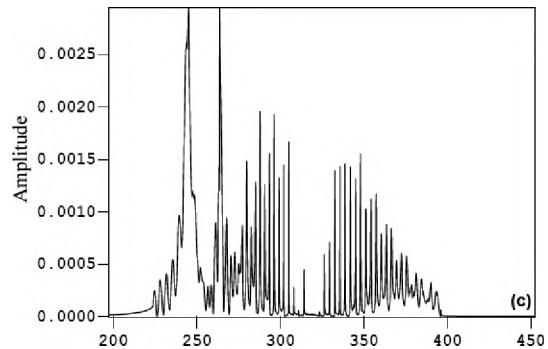


Figure 10 (c) Resulting Resonance Spectra of the symmetric S_1 wave

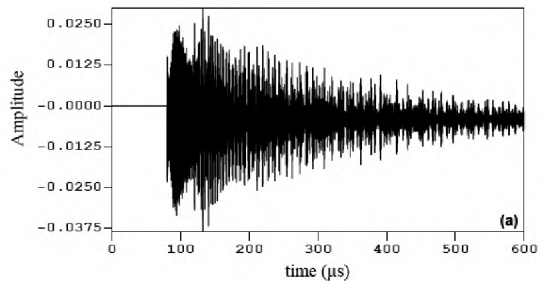


Figure 11 (a) Time Signal of the antisymmetric A_2 wave

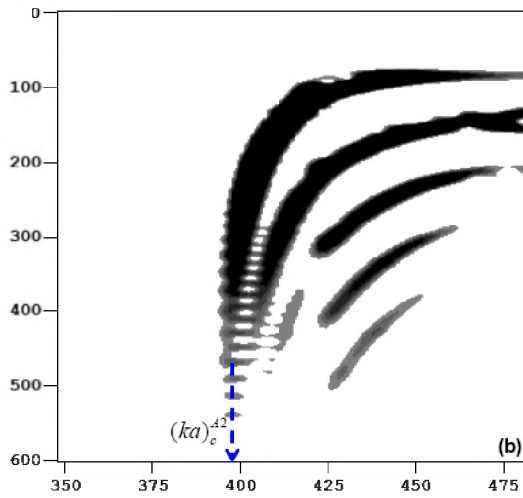


Figure 11 (b) Spectrometric Image of the antisymmetric A_2 wave

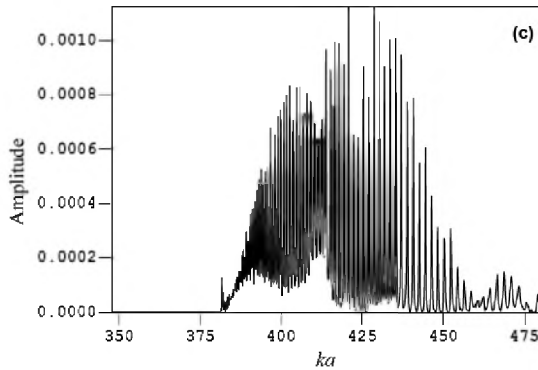


Figure 11 (c) Resulting Resonance Spectra of the antisymmetric A_2 wave

4. RESULTS

4.1 Cut-off Frequency

The spectrogram images in Figures 9, 10 and 11, show clearly the evolution of the antisymmetric A_1 , symmetric S_1 (with $m=2$) and antisymmetric A_2 waves, on the time-frequency plane (remark 31) respectively (the reduced frequencies ranges are $ka > 132$, $200 < ka < 400$ and $395 < ka < 500$ respectively). With increasing time, the trajectory associated with these different waves tends to asymptotic values which equal the reduced cut-off frequencies $(ka)_c^{A_1}$, $(ka)_c^{S_1}$ and $(ka)_c^{A_2}$ respectively. This reduced cut-off frequencies are the intersection points of the wave's asymptotic trajectories and the reduced frequency axis.

The recorded values are,

$$(ka)_c^{A_1} = 132.0 \pm 0.8 \text{ (Fig. 9b),}$$

$$(ka)_c^{S_1} = 264.7 \pm 0.5 \text{ (Fig. 10b) and,}$$

$$(ka)_c^{A_2} = 396.3 \pm 0.8 \text{ (Fig. 11b).}$$

The comparison between the results obtained by the time-frequency spectrogram method and the other method mentioned above (Table 2) are in good agreement. The following table summarizes the comparison between the various methods results.

Table 2. Comparison between the obtained results

Wave type	Lamb wave		Circumferential waves
	$fe/2(\text{Mhz mm})$	Ka	ka (spectrogram method)
A_1	0.775 ± 0.020	132.5 ± 3.41	132 ± 0.5
S_1	1.550 ± 0.020	264.8 ± 3.41	264.7 ± 0.5
A_2	2.325 ± 0.020	397.5 ± 3.41	396.3 ± 0.5

4.2 Transverse and Longitudinal Velocities

For the antisymmetric A_1 and A_2 waves (with $m=1$ and $m=3$ respectively), the transverse velocity, of the aluminum material of the tube, determined by the Spectrogram images (Fig 9.b and 11.b respectively) are $C_T = 3088 \pm 18.0$ m/s and $C_T = 3090.6 \pm 18.0$ m/s respectively.

For the symmetric S_1 wave (with $m=2$), the longitudinal velocity estimated by the Spectrogram image (Fig 10.b) is $C_L = 6192.8 \pm 9.0$ m/s. Moreover, we note that the transverse velocities estimated by the antisymmetric A_1 and A_2 waves and the longitudinal velocity obtained by the symmetric S_1 wave agree with those given by the normal mode [13,30,36,41] ($C_T = 3100$ m/s and $C_L = 6380$ m/s).

5. CONCLUSIONS

The time-frequency spectrogram representation can be utilized as a good technique for characterizing a thin elastic tube. The characterization consists in determining different parameters such as the cut-off frequencies, the longitudinal and transverse velocities. This representation gives a good energy distribution in the time-frequency plane. The spectrogram images allow identifying the circumferential waves propagating around the tube circumference, and follow the evolution of the frequency contents of each circumferential wave with respect to time. This representation allows us to determine, with precision, the cut-off frequencies of the A_1 , S_1 and A_2 waves. The comparison between the cut-off frequencies obtained from the spectrogram images and those calculated theoretically by the normal modes theory are in good agreement. Thus, we can consider measurements of the cut-off frequencies in situations

where theoretical results are not available. Moreover, in the majority of composite materials (very complex structures), the prediction of the circumferential waves characteristics from theory is almost impossible. However, one can easily measure them by using the spectrogram time-frequency representation. Finally this representation permits the determination of the transverse and longitudinal velocities of an aluminum tube. The results of the velocities are seen to be in good agreement with those measured by earlier experimental methods found in the literature.

REFERENCES

1. P. L. Marston and N. H. Sun, "Backscattering near the coincidence frequency of a thin cylindrical shell: surface wave properties from elastic theory and an approximate ray synthesis", *J. Acoust. Soc. Am.* vol. 97, pp. 777-783, 1995.
2. G. Maze, F. Léon, N. Veksler, L. Ripoche, "Resonance identification of a solid axisymmetric finite length target" *J. Acoust. Soc. Am.* 95, 3000, 1994.
3. Farid Chati, Fernand Léon, Gérard Maze, "Acoustic scattering by a metallic tube with a concentric solid polymer cylinder coupled by a thin water layer. Influence of the thickness of the water layer on the two Scholte-Stoneley waves" *J. Acoust. Soc. Am.* 118 2820, 2005.
4. S. F. Morse and P. L. Marston, "Backscattering of transients by tilted truncated cylindrical shells: Time-frequency identification of ray contributions from measurements", *J. Acoust. Soc. Am.* vol. 111, pp. 1289-1294, 2002.
5. G. Maze D. Décultot, A. Klauson, J. Metsaveer, "Acoustic scattering by immersed circular cylindrical shell stiffened by internal lengthwise rib" *J. Acoust. Soc. Am.* 95 2868, 1994.
6. G. Maze, F. Lecroq, D. Décultot, J. Ripoche, Sus an K. Numrich, H. Überall, "Acoustic scattering from finite cylindrical elastic objects" *J. Acoust. Soc. Am.* 90 3271, 1991.
7. G. Maze, J. Ripoche, Xiao-Ling Bao, H. Überall, "Acoustic scattering from elastic cylinders" *J. Acoust. Soc. Am.* 89 1993, 1991.
8. D. Décultot, F. Lecroq, G. Maze, J. Ripoche, "Acoustic scattering from immersed axisymmetric objects. Cylindrical shell limited by hemispherical encaps" *J. Acoust. Soc. Am.* 95, 3000, 1994.
9. G. Maze, "Acoustic scattering from submerged cylinders. MIIIR Im/Re: Experimental and theoretical study", *J. Acoust. Soc. Amer.*, vol. 89, pp. 2559-2566, 1991.
10. M. Castaings, P. Cawley, "The generation, propagation and detection of Lamb waves in plates using air-coupled ultrasonic transducers" *J. Acoust. Soc. Am.* 100, 3070, 1996.
11. N. H. Sun and P. L. Marston, "Ray synthesis of leaky Lamb wave contributions to backscattering from thick cylindrical shells", *J. Acoust. Soc. Am.* vol. 91, pp. 1398-1402, 1992.
12. M. Talmant, G. Quentin, J.L. Rousselot, J.V. Subrahmanyam, and H. Ubreall, "Acoustic resonances of thin cylindrical shells and the resonance scattering theory", *J. Acoust. Soc. Am.* 84(2), 681-688, 1988.
13. R. Latif, E. Aassif, A. Moudden, D. Decultot, B. Faiz, G. Maze, "Determination of the cut-off frequency of an acoustic circumferential wave using a time-frequency analysis", *NDT&E International* 33, 373-376, 2000.
14. L. Cohen, "Time-frequency analysis", Prentice Hall, New Jersey, 1995.
15. P. Flandrin, "Temps-fréquence", Hermès, Paris, 1993.
16. N. Yen, R. Dragonette Louis, K. Numrich Susan, "Time-frequency analysis of acoustic scattering from elastic objects", *J. Acoust. Soc. Am.* 87(6), 2359-2370, 1990.
17. F. Léonard, "Spectrogramme de phase et spectrogramme de fréquence", *Revue du Traitement du Signal* 17 (4), 269-286, 2001.
18. M. Niethammer, L.J. Jacobs, J. Qu, J. Jarzynski, "Time-frequency representation of Lamb waves using the reassigned spectrogram", *J. Acoust. Soc. Am.* 107, 19-24, 2000.
19. P. Flandrin, J. Sagéoli, J. P. Sassarego and M. E. Zakharia "Application of time-frequency analysis to the characterization of surface waves on elastic targets", *Acoustics letters* vol. 10, pp 23-28, 1986.
20. R. Latif, E. Aassif, A. Moudden, B. Faiz, G. Maze, "The experimental signal of a multilayer structure analysis by the time-frequency and spectral methods", *Journal of Non Destructive Testing & Evaluation International*, Vol. 39, 349-355, 2006.
21. R. Latif, E. Aassif, A. Moudden, B. Faiz, "High-resolution time-frequency analysis of an acoustic signal backscattered by a cylindrical shell using a modified Wigner-Ville representation", *Meas. Sci. Technol.* 14, 1063-1067, 2003.
22. R. Latif, E. H. Aassif, G. Maze, A. Moudden, B. Faiz, "Determination of the group and phase velocities from time-frequency representation of Wigner-Ville", *Journal of Non Destructive Testing & Evaluation International*, Vol. 32, 7, 415-422, 1999.
23. Viktorov, I.A., "Rayleigh-type waves on a cylindrical surface", *Soviet Phys.-Acoust.*, 4, 131-136, 1958.
24. Qu, J., Berthelot, Y., and Li, Z., "Dispersion of guided circumferential waves in circular annulus", *Rev. Prog. Quant. Nondestructive Evaluation*, 15, 169-176, 1996.
25. Liu, G. and Qu, J., "Guided circumferential waves in a circular annulus", *J. Appl. Mech.*, 65, 424-430, 1998a.
26. Cerv, J., 1988, "Dispersion of elastic waves and rayleigh-type waves in a thin disc", *Acta Technica Csav*, 89, 89-99, 1988.

27. Mindlin, R.D., and McNiven, H.D., "Axially symmetric waves in elastic rods", J. Appl. Mech., 82, 145-151, 1960.
28. Pao, Y.H. and Mindlin, R.D., "Dispersion of flexural waves in an elastic, circular cylinder", J. Appl. Mech., 27, 513-520, 1960.
29. N. D. Veksler, M. E. Kutser, "Asymptotics of the pressure field in a specific discontinuity for diffraction of a plane acoustic wave on an elastic cylindrical shell", Journal of Applied Mathematics and Mechanics, Volume 40; Issue 3, Pages 464-474, 1976.
30. R. Latif, E. Aassif, G. Maze, D. Decultot, A. Moudou and B. Faiz, Analysis of the circumferential acoustic waves backscattered by a tube using the time-frequency representation of Wigner-Ville", Meas. Sci Technol. 11 pp. 83-88, 2000.
31. D. Gabor. "Theory of communication", Journal of the Institute for Electrical Engineers, 93:429-439, 1946.
32. M. Destrade, Explicit secular equation for Scholte waves over a monoclinic crystal, Journal of Sound and Vibration 273 (2004) 409-414.
33. J.B. Allen and L.R. Rabiner. "A unified approach to STFT analysis and synthesis", Proceedings of the IEEE, 65:1558 - 1564, November 1977
34. F. Magand, P. Chevret, "Time-frequency analysis of energy distribution for circumferential waves on cylindrical elastic shells" acta acoustica, Vol. 82, pp. 707-716, 1996.
35. J.P. Sessarego, J. Saheloli, P. Degoul, P. Flandrin, M. Zakharia "analyse temps-fréquence des signaux en milieux dispersifs. Application à l'étude des ondes de Lamb" J. Acoustique 3, pp. 273-280, 1990.
36. G. Maze, J.L. Izbicki, J. Ripoché, "Resonances of plates and cylinders: Guided waves ", J. Acoust. Soc. Amer. vol 77, pp. 1352-1357, 1985.
37. J. Qu, L. Jacobs, "Cylindrical Waves and Their Applications in Ultrasonic Evaluation," in Ultrasonic NDE for Engineering and Biological Material Characterization, ed. T.Kundu, CRC Press, p.311- 36, 2004.
38. R. Fiorito, W. Madogosky, H. Überall, "Theory of ultrasonic resonances in viscoelastic layer", J. Acoust. Soc. Am. Vol. 77, No. 2, February, 489-498, 1985.
39. R. Fiorito, W. Madogosky, H. Überall, "Resonance theory of acoustic waves interacting with an elastic plate", J. Acoust. Soc. Am. Vol. 66, No. 6, December, 1857-1866, 1979.
40. L. Derbesse, P. Pernod, V. Latard, A. Merlen, D. Décultot, N. Touraine, G. Maze, "Acoustic scattering from complex elastic shells: visualization of S0,A0 and A waves", Ultrasonics, Volume 38, Issue 1-8, March Pages 860-863, 2000.
41. P.L. Marston and N.H. Sun, " Backscattering near the coicidance frequency of a thin cylindrical shell: surface wave properties from elastic theory and an approximate ray synthesis", J. Acoust. Soc. Am. vol 97, pp. 777-783, 1995.



Freedom Step

Convert a standard floor to a superior floor with the Freedom Step Acoustical & Impact Isolation Subfloor

AcustiFloat®
Acoustical & Impact Subfloor Systems

WILREP LTD.
Tel. (905) 625-8944 Toll Free 1-888-625-8944
www.acustifloat.com



Gym Rooms Playrooms Home Theaters Dance Floors

AcustiFloat is a registered Trademark of WILREP LTD.